

VIP Very Important Paper

Special
Collection

Regiodivergent Synthesis of Benzothiazole-Based Isosorbide Imidates by Oxidative N-Heterocyclic Carbene Catalysis

Daniele Ragno,^[a] Carmela De Risi,^[a] Alessandro Massi,^[a] Graziano Di Carmine,^[a] Sofia Toldo,^[a] Costanza Leonardi,^[a] and Olga Bortolini^{*[b]}

Dedicated to Professor Cesare Gennari on the occasion of his 70th birthday.

A novel N-heterocyclic carbene (NHC)-promoted regiodivergent protocol for *exo* (2-OH) and *endo* (5-OH) isosorbide (IS) imidates synthesis is described. The disclosed strategy allows the straightforward synthesis of monoimidate-isosorbides (MIIIs) endowed with the biologically relevant benzothiazole (BTA) moiety under mild oxidative conditions, starting from easy-accessible aldimines. Process optimization encompassed the use of stoichiometric diquinone as well as atmospheric oxygen as oxidant species, focusing on reaction dichotomy between oxidative and oxygenative pathways. The reaction scope was investigated on a representative selection of BTA-containing

aldimines and further extended to congeners bearing different biologically pivotal N-heterocyclic rings (benzoxazole, thiazole and isoxazole), observing good levels of yield (up to 87%) and regioselectivity (*exo/endo* up to 10.0; *endo/exo* up to 7.0). Furthermore, the employment of an immobilized-NHC under heterogeneous conditions was assessed, showing satisfactory selectivity towards *exo*-MIIIs (*exo/endo*=3.8). Overall, the methodology presented provided an unprecedented collection of high value-added products with potential applications in different fields.

Introduction

Benzothiazole (BTA) ring system is a common heterocyclic scaffold in many natural and/or synthetic products with proven biological and pharmacological properties,^[1,2] such as antimicrobial, fungicide, anticancer, antioxidant, anti-inflammatory, analgesic, antiviral, anticonvulsant, antitubercular, antidiabetic, antileishmanial, antihistaminic, antimalarial, antidepressant, as well as enzyme and receptor agonists/antagonists. Other than this, some BTA derivatives proved active against neurodegenerative diseases.^[3]

As cases in point, Erythrazole B is a typical example of a naturally occurring BTA derivative showing cytotoxicity against diverse non-small cell lung cancer (NSCLC) cell lines,^[4] while

synthetic BTA-sulfonamides have demonstrated effective activity against Gram positive bacteria.^[5] Riluzole is currently marketed for the treatment of amyotrophic lateral sclerosis (ALS),^[6] Pittsburgh compound B is used as a positron emission tomography (PET) imaging agent for Alzheimer's disease (AD),^[7] and Benthivalicarb-isopropyl^[8] is a commercially available fungicide (Figure 1).

Something that is equally remarkable is the key role that BTA compounds may play in the area of functional materials.^[9]

Seeing the value of BTA derivatives, the development of novel synthetic methods to access BTA-based compounds remains valuable.^[10] In this context, N-heterocyclic carbene (NHC) catalysis represents a suitable strategy for the preparation

[a] Dr. D. Ragno, Dr. C. De Risi, Prof. A. Massi, Dr. G. Di Carmine, S. Toldo, C. Leonardi

Department of Chemical, Pharmaceutical and Agricultural Sciences
University of Ferrara
Via L. Borsari, 46, 44121 Ferrara, Italy

[b] Prof. O. Bortolini

Department of Environmental and Prevention Sciences
University of Ferrara
Via L. Borsari, 46, 44121 Ferrara, Italy
E-mail: olga.bortolini@unife.it
http://docente.unife.it/olga.bortolini

Supporting information for this article is available on the WWW under <https://doi.org/10.1002/ejoc.202200482>

Part of the "DCO-SCI Prize and Medal Winners 2020/2021" Special Collection.

© 2022 The Authors. European Journal of Organic Chemistry published by Wiley-VCH GmbH. This is an open access article under the terms of the Creative Commons Attribution Non-Commercial NoDerivs License, which permits use and distribution in any medium, provided the original work is properly cited, the use is non-commercial and no modifications or adaptations are made.

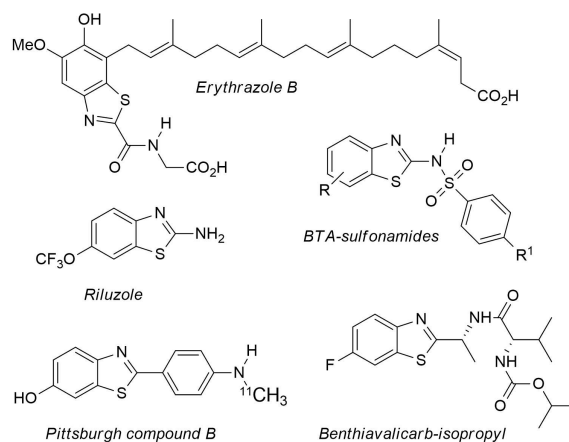


Figure 1. Representative examples of biologically relevant BTA derivatives.

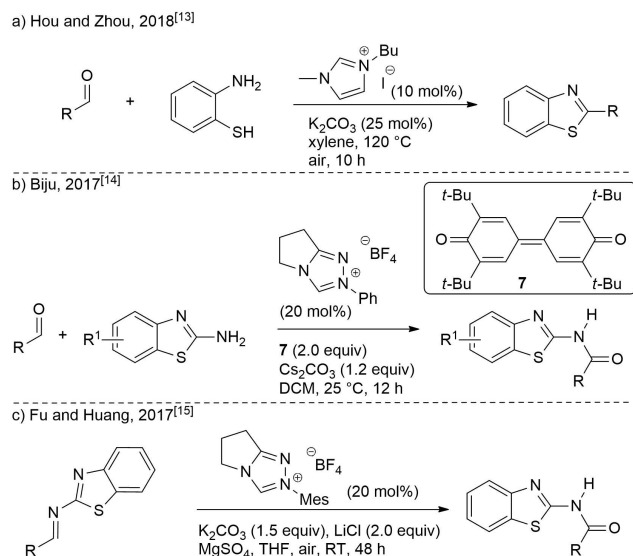
of molecules endowed with a BTA moiety. Thus, BTA-based α -aminoketones were conveniently prepared by Chi *et al.* through NHC-catalyzed *aza*-benzoin reaction between *N*-sulfonylimines and benzothiazole-2-carboxaldehydes.^[11]

In the field of oxidative NHC-catalysis,^[12] 2-substituted benzothiazole compounds were conveniently assembled from 2-aminobenzethiol and aldehydes under aerobic conditions (Scheme 1a).^[13] Direct oxidative amidation of aldehydes with 2-aminobenzothiazoles in the presence of Kharasch oxidant **7** was reported by Biju group (Scheme 1b),^[14] while Huang *et al.* described a LiCl-assisted aerobic route to BTA amides from 2-aminobenzothiazole-derived imines (Scheme 1c).^[15]

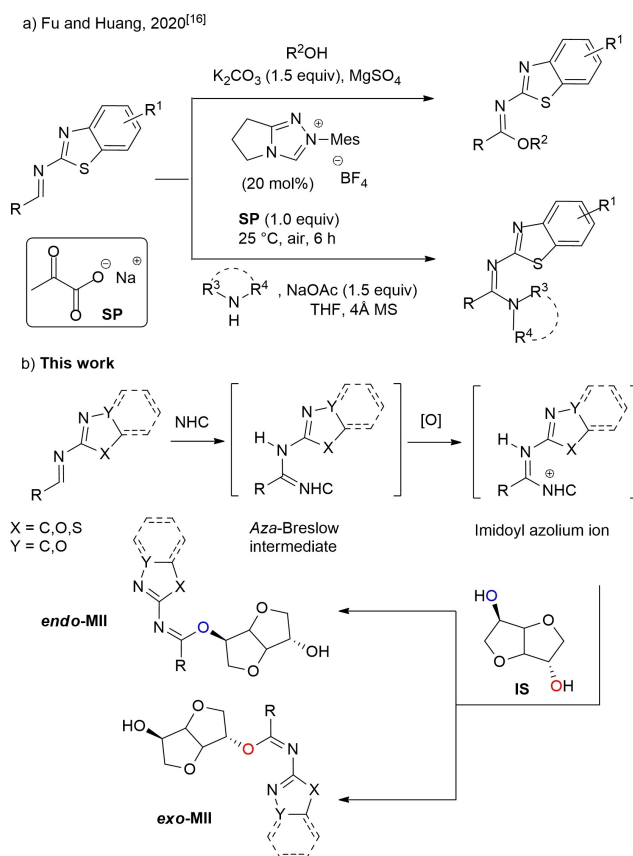
2-Aminobenzothiazole-derived imines were further employed in aerobic oxidative reactions with alcohols and amines paving the way to the preparation of BTA-containing imidates and amidines, respectively (Scheme 2a).^[16] This strategy features the use of sodium pyruvate (SP) as a novel peroxide scavenger to selectively address the reaction pathway towards the oxidative one. Importantly, the imidate and amidine motifs are found in pharmaceutically relevant molecules,^[17] in addition to being key synthons for a number of synthetic transformations.^[18] In particular, BTA-functionalized imidates and amidines may find application as ligands in metal catalysis and fluorescent dyes due to their peculiar structural and electronic features.^[19]

On these grounds and inspired by our continuous interest in biomass valorization through organocatalytic processes,^[20] we anticipated that conjugation of a bio-based feedstock with the biologically relevant BTA and/or imidate (amidine) moieties would allow high value-added products for possible use in the typical fields of application of either benzothiazoles or imidates (amidines).

A typical bio-based platform chemical is isosorbide (IS, 1,4:3,6-dianhydro-D-glucitol or 1,4:3,6-dianhydrosorbitol), a GRAS (generally recognized as safe) renewable diol industrially



Scheme 1. Synthetic approaches to 2-substituted BTA compounds and BTA amides via oxidative NHC-catalysis.



Scheme 2. NHC-catalyzed oxidative strategy to access BTA-containing imidates (amidines) (a) and this work (b).

obtained from glucose *via* a hydrogenation/dehydration route.^[21] IS is constituted by two *cis*-fused tetrahydrofuran rings (V-shaped molecule) appended with two nonequivalent secondary hydroxyl groups in *endo* (5-OH) and *exo* (2-OH) configurations (Figure 2), having different chemical behaviour: due to intramolecular hydrogen bonding with the oxygen atom of the opposite tetrahydrofuran ring, the *endo*-5-OH is a better nucleophile than the *exo*-2-OH, while being more sterically hindered.^[22] IS has been widely used as the key precursor for the manufacturing of diverse high value-added derivatives,

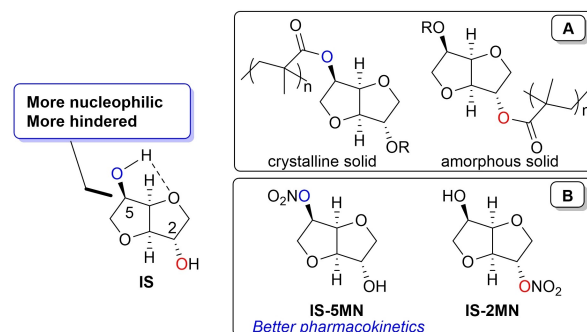


Figure 2. Structure of IS and its representative monoprotected derivatives.

including catalysts,^[23] polymers,^[24] plasticizers,^[25] surfactants,^[26] as well as pharmaceuticals.^[27]

In this respect, the preparation of IS-based compounds often goes through the regioselective functionalization of the 2- and 5-hydroxyl groups, as the corresponding *exo*- and *endo*-derivatives are expected to display different physicochemical and biological properties. As a matter of fact, regioisomeric IS-derived vinyl monomers have been shown to provide polymers with different physical properties (Figure 2A),^[28] while the clinically used isorbide-5-mononitrate (IS-5MN) displays a better pharmacokinetics compared to isorbide-2-mononitrate (IS-2MN) (Figure 2B).^[29]

Recently, we have demonstrated that oxidative NHC-catalysis can be efficiently used as the organocatalytic platform for the regiodivergent monoacylation of IS with aldehydes at either the *endo*- and *exo*-positions, using diquinone **7** as the oxidant.^[20e] In continuation of this work and inspired by the studies of Fu and Huang (Scheme 2a),^[16] we speculated that isorbide could be utilized as a nucleophile in NHC-catalyzed oxidative reactions with 2-aminobenzothiazole-derived aldi-

mines (Scheme 2b). We report herein the results of our investigations, which gave access to a library of unprecedented BTA-based *endo*- and *exo*-monoimide-isosorbides (MIIIs) with good yields and regioselectivities. It is highlighted that the developed methodology has proved to be very versatile, being effectively extended to aldimines containing *N*-heterocyclic rings other than benzothiazole (i.e. benzoxazole, thiazole, isoxazole). Notably, the great structural variability that can be obtained at the imine level allows isorbide to be endowed with extremely varied imide functions, which could be useful in terms of new drug/materials design and synthesis.

Results and Discussion

The regioselective synthesis of monoimides **3a** and **4a** starting from isorbide **2** and aldimine **1a** was selected as the benchmark, using diquinone **7** as stoichiometric oxidant and a suitable base for pre-catalysts **A-C** activation (Table 1). Our investigation started from reaction conditions which revealed

Table 1. Optimization Study with Diquinone **7** as Oxidant.^[a]

Entry	NHCHX [mol %]	Base [mol %]	Solvent	t [h]	3a [%] ^[b]	4a [%] ^[b]	5a [%] ^[b]
1	A (20)	DBU (30)	THF	3	41	30	/
2	A (20)	DBU (30)	DCM	1	85	15	/
3	A (10)	DBU (25)	DCM	1.5	85	15	/
4	A (5)	DBU (20)	DCM	3	85	13	/
5	B (20)	Et ₃ N (30)	DMSO	2	30	53	5
6	B (20)	DBU (30)	DMSO	3.5	43	57	/
7	B (20)	Et ₃ N (30)	DMF	3	47	53	/
8	B (20)	DBU (30)	DMF	2	24	67	9
9	B (10)	DBU (25)	DMF	3	20	75	5
10	B (5)	DBU (20)	DMF	5	27	62	/
11	B (10)	DBU (25)	DMA	24	23	42	/
12	B (10)	DBU (25)	NMP	6	14	75	/
13	A (10)	DBU (25)	NMP	5	33	57	10
14	B (10)	DBU (25)	DCM	5	75	23	2
15	C (10)	DBU (25)	NMP	6	31	61	8
16	C (10)	DBU (25)	DCM	5	71	19	/
17	D (10)	DBU (25)	DCM	6	75	20	/

A **B** **C**

D (f: 0.42 mmol g⁻¹) **7** **7***

[a] **1a** (0.20 mmol), **2** (0.60 mmol), anhydrous solvent (2.0 mL). [b] Detected by ¹H NMR of the crude reaction mixture with duren as the internal standard.

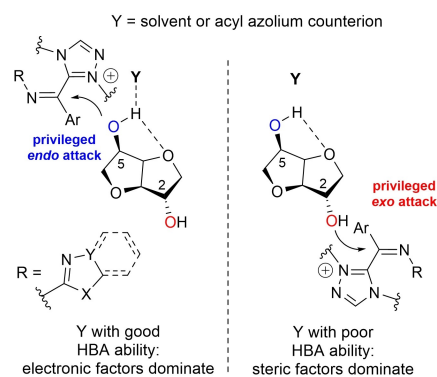
to be effective for the *exo*-selective acylation of IS,^[20e] using a three-fold excess of IS to minimize the formation of diimidate byproduct **5a**. Reaction run in anhydrous THF, at room temperature, using triazolium salt **A** (20 mol%) in combination with 1,8-diazabicyclo[5.4.0]undec-7-ene (DBU) led, after 3 hours, to partial aldimine conversion with low regioselectivity (*exo*-MII **3a**, 41%; *endo*-MII **4a**, 30%. Entry 1). Solvent change to DCM led to full conversion and improved regioselectivity, reducing reaction time (*exo*-MII **3a**, 85%; *endo*-MII **4a**, 15%. Entry 2). Excellent levels of conversion and selectivity were retained lowering the pre-catalyst loading up to 5 mol% (entries 3–4), representing the best conditions for the synthesis of *exo*-derivatives (*exo*-MII **3a**, 85%; *endo*-MII **4a**, 13%. Entry 4). At this stage of the study, the reaction conditions towards the selective synthesis of *endo*-MII **4a** were screened. In our previous contribution,^[20e] we observed that the selectivity towards *endo*-IS monoesters was mainly favored by solvents with strong hydrogen-bond-accepting (HBA) character, due to 5-OH nucleophilicity enhancement by intermolecular hydrogen bonding interactions. These findings prompted us to evaluate the solvent effect in the synthesis of IS-imidates, using DMSO and pre-catalyst **B** (20 mol%), which was found to be the most effective combination for *endo*-acylations. A selectivity switch to *endo*-MII **4a** was observed under these conditions, using both Et₃N and DBU (entries 5–6) as bases.

The replacement of DMSO with DMF (entries 7–8) afforded poor selectivity using Et₃N as the base and enhanced regioselectivity using DBU, although low amounts of byproduct **5a** were detected (*exo*-MII **3a**, 24%; *endo*-MII **4a**, 67%; **5a**, 9%. Entry 8). Reduction of pre-catalyst loading to 10 mol% led to increased selectivity (*exo*-MII **3a**, 20%; *endo*-MII **4a**, 75%. Entry 9), while further decrease to 5 mol% resulted in longer reaction time with slight regioselectivity erosion (entry 10). Next, we wondered if the use of DMF-like solvents could improve the process regioselectivity. For this reason, DMA and NMP were screened, leading to longer reaction time and low selectivity for the former (*exo*-MII **3a**, 23%; *endo*-MII **4a**, 42%. Entry 11), and excellent *endo* selectivity for the latter (*exo*-MII **3a**, 14%; *endo*-MII **4a**, 75%. Entry 12). As a result, the reaction conditions highlighted in Entry 12 (Table 1) were the most performing for *endo*-derivatives production. In order to gain more insights on the regioselective control, catalyst and solvent effect was investigated. Pre-catalysts **A** and **B** were respectively screened in NMP (entry 13) and DCM (entry 14), which were selected as the best solvents for *endo*- and *exo*-MII production. As a result, triazolium salt **A** showed *endo*-selectivity in NMP, while pre-catalyst **B** led to preferential formation of *exo*-MII **3a** in DCM. A clear selectivity switch was observed moving from DCM to NMP for pre-catalyst **A** (entry 3 vs entry 13) and **B** (entry 14 vs entry 12), confirming the strong influence of solvent hydrogen-bond-accepting (HBA) character on the regioselectivity. As reported in our previous contribution,^[20e] it can be hypothesized that the reaction preferentially occurs at the less sterically hindered *exo*-2-OH in solvents with poor HBA character because of the intrinsic bulkiness of the imidoyl azolium intermediates, while involvement of the more nucleophilic *endo*-5-OH occurs when intermolecular hydrogen-bond-

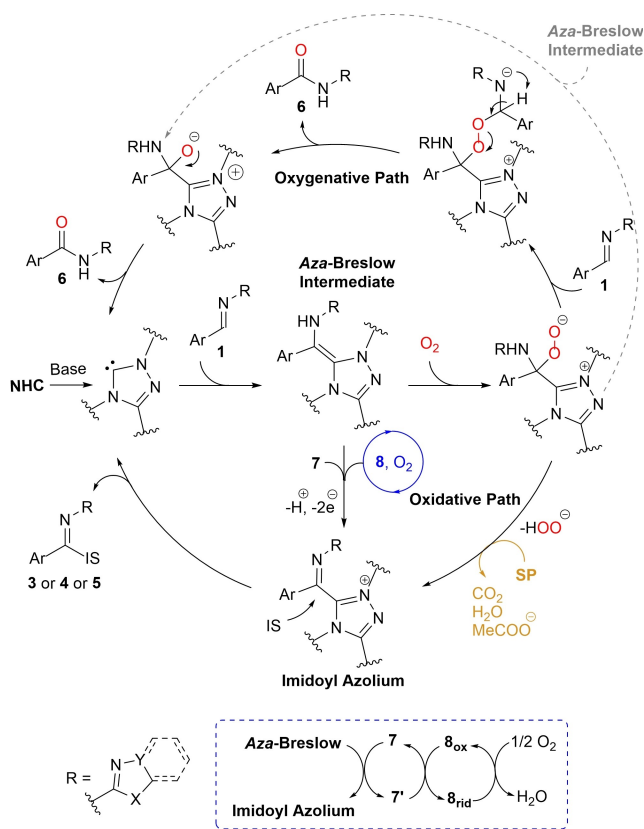
ing interactions are activated by the presence of a suitable coordinating solvent and/or counterion (Scheme 3). At the same time, catalyst effect was less determining, but not negligible. Indeed, under the same reaction conditions (entry 3 vs entry 14 and entry 12 vs entry 13), triazolium salt **A** was more selective towards *exo*-MII while **B** was more selective towards *endo*-derivatives. Finally, the observed solvent/catalyst effect trend was confirmed in the screening of mesityl-substituted pre-catalyst **C**, which afforded preferentially *endo*-MII **4a** in NMP (entry 15) and *exo*-MII **3a** in DCM (entry 16) with lower levels of selectivity.

Once established the optimized regiodivergent conditions for the homogeneous process, the utilization of a heterogeneous immobilized NHC was considered. NHC immobilization typically enables for easy catalyst separation/recycling and may limit carbene deactivation caused by air and moisture, therefore enhancing the overall productivity and sustainability of the process.^[30] For these reasons, the polystyrene-supported pre-catalyst **D** was prepared, starting from commercial Merrifield resin, according to literature procedure.^[20b] The immobilized triazolium salt revealed to be highly active and selective towards *exo*-MIIs (*exo*-MII **3a**, 75%; *endo*-MII **4a**, 20%. Entry 17), affording similar results compared to its homogeneous counterpart (pre-catalyst **A**), with longer reaction time. Although satisfactory levels of regioselectivity were achieved using the immobilized pre-catalyst, the homogeneous process was faster and more selective (entry 4).

With the optimized regiodivergent conditions in our hands, the use of air as terminal oxidant was considered. As shown in Scheme 4, under aerobic conditions two competitive reaction pathways, oxidative and oxygenative, coexist.^[16,31] The former leads to target IS-imidate while the latter affords undesired amide **6**, therefore an efficient strategy for suppression of the oxygenative route is needed. In details, oxidative pathway can proceed *via* direct oxidation of *aza*-Breslow intermediate by diquinone **7**^[32] or through nucleophilic addition of the *aza*-Breslow species to O₂, forming a peroxidic species which is in turn converted to the imidoyl azolium after removal of the peroxide moiety, as recently reported by Fu and Huang (Scheme 4, orange pathway).^[16] Final nucleophilic attack of IS to the electrophilic imidoyl azolium affords the target imidate



Scheme 3. Tentative rationalization of the origin of regioselectivity in NHC-catalyzed IS-imidates synthesis (HBA: Hydrogen-Bond-Accepting).



Scheme 4. Proposed mechanism for NHC-oxidative synthesis of IS-imidates and amides **6** respectively through oxidative and oxygenative pathways.

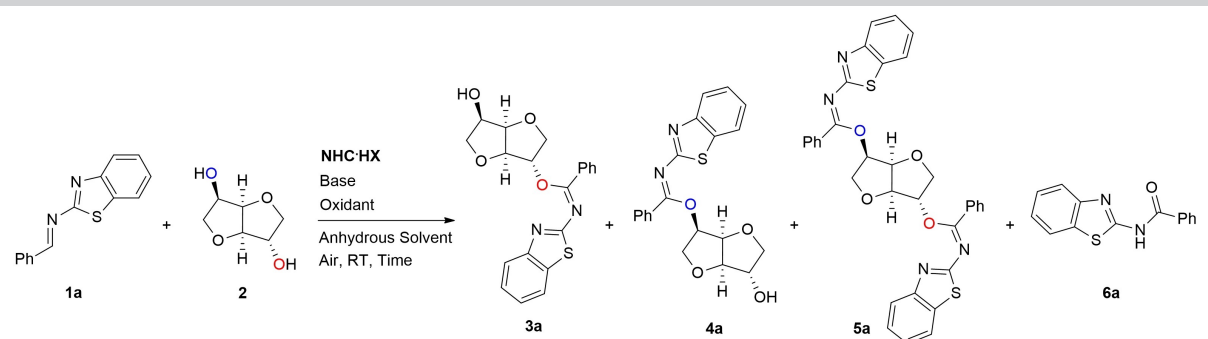
compound. Differently, oxygenative pathway goes through the nucleophilic addition of the peroxidic intermediate to another molecule of aldimine **1**, affording finally two molecules of amide **6**.^[15,16] An alternative oxygenative route calling for reduction of the peroxidic species by the *aza*-Breslow intermediate could not be ruled out, as reported in different works (Scheme 4, grey route).^[33] Notably, working under aerobic conditions required the addition of 4 Å molecular sieves, in order to remove water traces contained in atmospheric air which could hydrolyze the starting aldimine and compete with IS nucleophilic attack.

Based on these premises, the aerobic process was optimized (Table 2). First, the biomimetic system of electron-transfer mediators (ETMs) developed by Bäckvall^[34] and Sundén^[35] groups was tested in the model reaction between imine **1a** and IS. By this strategy, imidoyl azolium formation is triggered by catalytic diquinone **7** (10 mol%), which is reduced to the corresponding diol **7'** (Scheme 4, blue box), next reoxidized to **7** by atmospheric oxygen in the presence of catalytic iron(II) phthalocyanine **8** (5 mol%).^[20a] In our first attempt, using pre-catalyst **A** (10 mol%) with DBU (25 mol%) in DCM, full imine conversion was detected after two hours, with good *exo*-selectivity (*exo*-MII **3a**, 77%; *endo*-MII **4a**, 16%. Entry 1) and little amounts of amide **6a** (5%). Reduction of pre-catalyst loading (entry 2) led to longer reaction time and lower conversion/selectivity, with formation of benzoic acid as by-

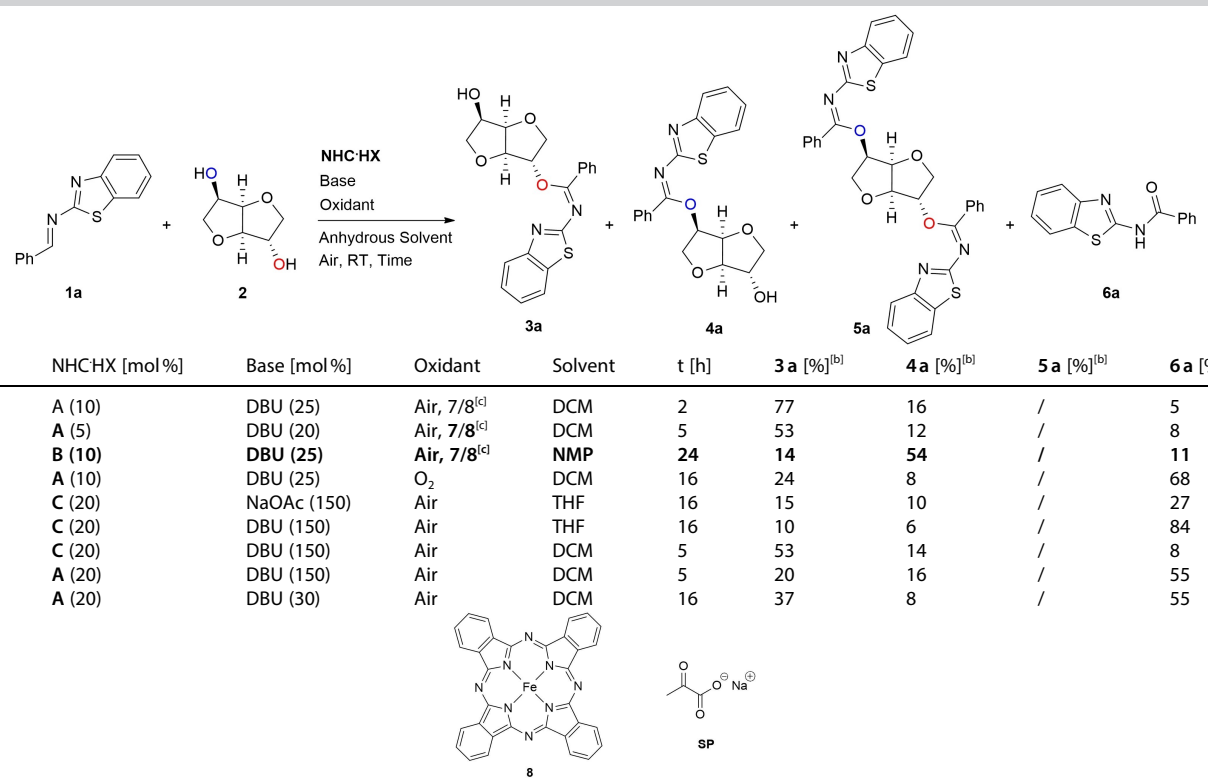
product (12%). This behavior could be ascribed to imine hydrolysis and subsequent NHC-oxidative promoted conversion of benzaldehyde into benzoic acid. ETMs system was also effective for selective *endo*-MII synthesis, employing pre-catalyst **B** (10 mol%) and DBU (25 mol%) in NMP (*exo*-MII **3a**, 14%; *endo*-MII **4a**, 54%. Entry 3), even though longer reaction time (24 h) was needed and increased formation of **6a** (11%) was detected. At this stage, the direct use of pure oxygen as sole oxidant (balloon technique, 1 bar) was evaluated, using pre-catalyst **A** (10 mol%) with DBU (25 mol%) in DCM (entry 4). Full imine conversion was observed after 16 h, with preferential formation of undesired amide **6a** (68%; entry 4), thus indicating a preferred reaction kinetics associated to the oxygenative pathway for the conversion of the *aza*-Breslow intermediate (Scheme 4). In order to favour the oxidative pathway over the oxygenative one, inspired by the recent publication by Fu and Huang (Scheme 2a),^[16] the use of stoichiometric sodium pyruvate (**SP**) as peroxide scavenger was assessed. According to this work, pyrrolidine-based pre-catalyst **C** (Cl⁻ salt instead of BF₄⁻ salt used by the authors) was tested in THF with different bases, showing poor *exo*-selectivity accompanied by important amounts of undesired amide **6a** (27%, entry 5; 84%, entry 6). Solvent change to DCM using DBU as the base allowed for better selectivity with substantial reduction of oxygenative byproduct (*exo*-MII **3a**, 53%; *endo*-MII **4a**, 14%; **6a**, 8%. Entry 7). Finally, pre-catalyst **A** screening led to negligible results using different amounts of base (entries 8–9).

Although promising results were achieved under aerobic conditions, especially using the ETMs system (entries 1, 3), the regiodivergent protocol based on the use of stoichiometric diquinone **7** (Table 1) was selected for the study of the reaction scope. In this regard, it is important to stress that diol **7'**, which is produced from diquinone **7** during the process, can be quantitatively reoxidized to **7** with air in the presence of catalytic phthalocyanine **8**, as detailed in the experimental section. Hence, the regioselective synthesis of IS-imidates was next examined with the representative classes of aldimines **1** to produce an unprecedented library of *exo*-MIIs and *endo*-MIIs. First, *exo*-derivatives were synthesized (Table 3) under the optimized conditions of Table 1 (entry 4), starting from aromatic 2-aminobenzothiazole-derived aldimines (**1a–f**). *o*-Chlorophenyl and *o*-methoxyphenyl BTA-imines afforded the corresponding *exo*-MIIs **3b,c** respectively with excellent and discrete yields. Selectivities were excellent in both cases, but increased amounts of competitive oxygenative byproduct **6c** (32%) were recorded for the *o*-methoxyphenyl substituted imine, probably due to longer reaction time (5 h). Imines bearing *para*-electron-withdrawing and *para*-electron-donating groups on the phenyl moiety (**1d,e**) revealed to be highly reactive, giving comparable levels of yield and regioselectivity, with traces of diimide **5d** (4%) in the first case and longer reaction time for **1e** (7 h). Prolonged reaction time (48 h) was needed also for the furanic imine **1f**, derived from biobased furfural, leading to *exo*-imidate **3f**. At this stage, the study was extended to imines containing different biologically relevant *N*-heterocycles (**1g–i**), widening the methodology versatility. 2-aminothiazole-derived imine **1g** afforded the corresponding *exo*-MII **3g** with 74% yield and *exo*-

Table 2. Optimization Study Under Aerobic Conditions.^[a]



Entry	NHC:HX [mol %]	Base [mol %]	Oxidant	Solvent	t [h]	3 a [%] ^[b]	4 a [%] ^[b]	5 a [%] ^[b]	6 a [%] ^[b]
1	A (10)	DBU (25)	Air, 7/8 ^[c]	DCM	2	77	16	/	5
2 ^[d]	A (5)	DBU (20)	Air, 7/8 ^[c]	DCM	5	53	12	/	8
3	B (10)	DBU (25)	Air, 7/8 ^[c]	NMP	24	14	54	/	11
4	A (10)	DBU (25)	O ₂	DCM	16	24	8	/	68
5 ^[e]	C (20)	NaOAc (150)	Air	THF	16	15	10	/	27
6 ^[e]	C (20)	DBU (150)	Air	THF	16	10	6	/	84
7 ^[e]	C (20)	DBU (150)	Air	DCM	5	53	14	/	8
8 ^[e]	A (20)	DBU (150)	Air	DCM	5	20	16	/	55
9 ^[e]	A (20)	DBU (30)	Air	DCM	16	37	8	/	55



[a] 1 a (0.20 mmol), 2 (0.60 mmol), anhydrous solvent (2.0 mL), 4 Å molecular sieves. [b] Detected by ¹H NMR of the crude reaction mixture with durene as the internal standard. [c] 7 (10 mol%), 8 (5 mol%). [d] Benzoic acid as byproduct (12% yield, NMR analysis). [e] SP (0.2 mmol) as peroxide scavenger.

endo = 6.1, while 2-aminobenzoxazole-derived *exo*-MII **3h** was obtained with the highest levels of yield and selectivity achieved (87% yield, *endo/exo* = 10.0). Finally, isoxazole-containing imine **1i** was poorly converted after 48 h with low selectivity.

Next, *endo*-MIIs reaction scope was investigated (Table 4), under the optimized conditions of Table 1 (entry 12). The same collection of starting aldimines was screened obtaining different values of reaction yield (58–80%) and regioselectivity (*endo/exo* = 7.0–2.0). These results were comparable to those of the benchmark reaction, apart from isoxazole-derivative **4i** which was produced with poor yield (12%) and selectivity (*endo/exo* = 1.8). The best results were collected for *o*-chlorophenyl substituted imine **1b**, which afforded MII **4b** with 80% yield and *endo/exo* = 7.0.

Conclusion

In summary, we have described the unprecedented regioselective synthesis of *endo*- and *exo*-monoimidate-isosorbides (MIIs) endowed with the biologically relevant BTA moiety through oxidative NHC catalysis. The disclosed strategy allowed for good levels of *endo*- and *exo*-selectivities with a representative selection of aldimines, and could be further extended to different biologically pivotal *N*-heterocyclic rings such as benzoxazole, thiazole and isoxazole. To the best of our knowl-

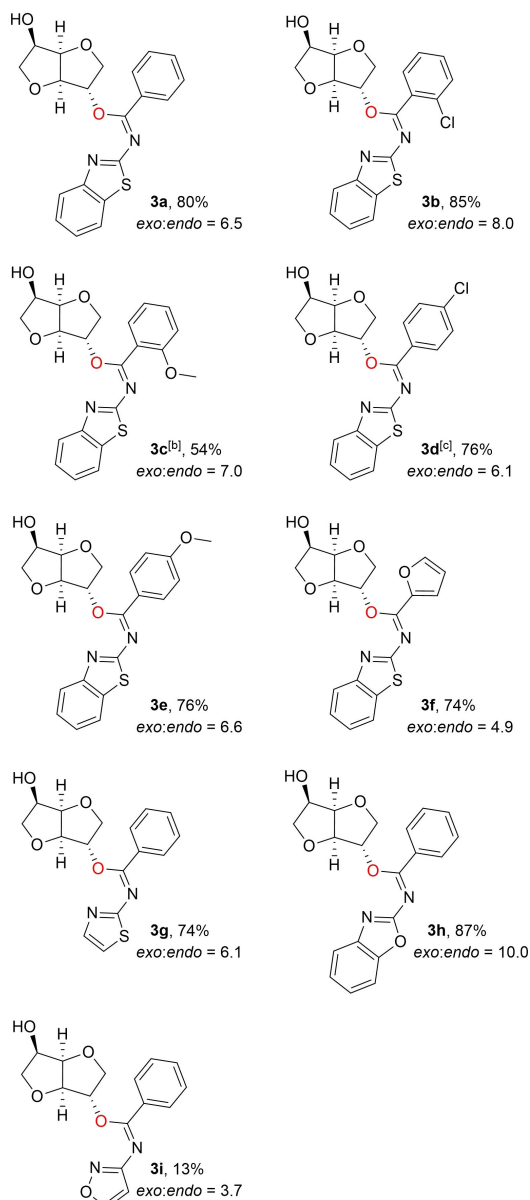
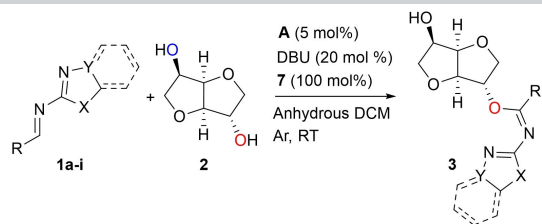
edge, this study represents the first example of regioselective straightforward functionalization of isosorbide with biologically relevant *N*-heterocyclic moieties. Bearing in mind the growing interest in feedstocks valorisation together with the central role of BTA and imidate motifs in the pharmaceutical and material fields, further investigations on physicochemical and biological properties of the synthesized library of *exo*- and *endo*-MIIs will be carried out in future studies, evaluating potential applications in different fields.

Experimental Section

General experimental conditions

All moisture-sensitive reactions were performed using oven-dried glassware under an Argon atmosphere. Anhydrous solvents were freshly distilled and dried over a standard drying agent prior to use. Reactions were monitored by TLC on silica gel 60 F₂₅₄ with detection with phosphomolybdic acid. Flash chromatography was performed on silica gel 60 (230–400 mesh). ¹H (300 MHz), ¹³C (101 MHz) NMR spectra were recorded in CDCl₃ at room temperature. The chemical shifts in ¹H and ¹³C NMR spectra were referenced to tetramethylsilane (TMS). Peak assignments were aided by ¹H-¹H COSY and gradient-HMQC experiments. For high resolution mass spectrometry (HRMS) the compounds were analyzed in positive ion mode using an Agilent 6520 HPLC-Chip Q/TOF-MS (nanospray) with a quadrupole, a hexapole, and a time of flight unit to produce the spectra. The capillary source voltage was

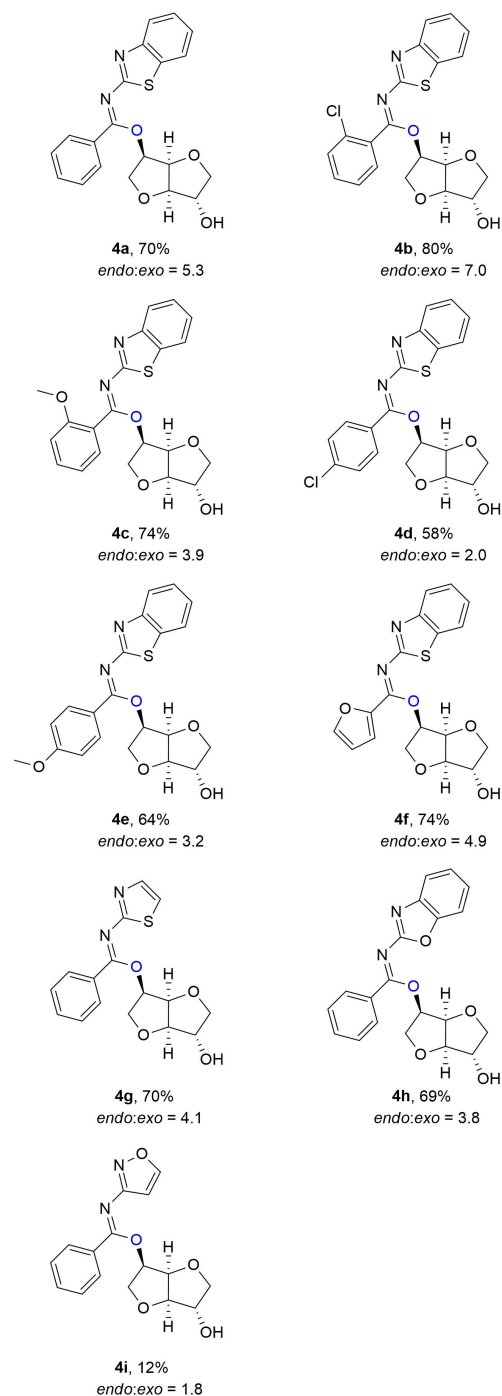
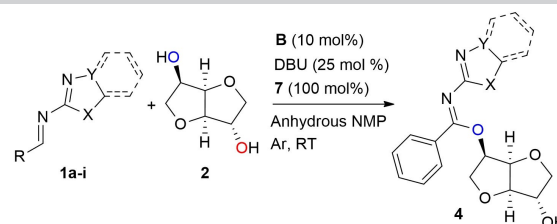
Table 3. Regioselective synthesis of *exo*-Mills 3 a–i.^[a]



[a] 1 a–i (0.20 mmol), 2 (0.60 mmol), anhydrous DCM (2.0 mL); isolated yields; selectivity detected by ¹H NMR of the crude reaction mixture. [b] Oxygenative byproduct 6c was isolated with 32% yield. [c] Diimidate 5d was isolated with 4% yield.

set at 1700 V; the gas temperature and drying gas were kept at 350 °C and 5 L min⁻¹, respectively. The MS analyzer was externally calibrated with ESI–L low concentration tuning mix from *m/z* 118 to 2700 to yield accuracy below 5 ppm. Accurate mass data were collected by directly infusing samples in 40/60 H₂O/ACN 0.1% TFA

Table 4. Regioselective synthesis of *endo*-Mills 4 a–i.^[a]



[a] 1 a–i (0.20 mmol), 2 (0.60 mmol), anhydrous NMP (2.0 mL); isolated yields; selectivity detected by ¹H NMR of the crude reaction mixture.

into the system at a flow rate of 0.4 $\mu\text{L min}^{-1}$. Elemental analyses were performed using a FLASH 2000 Series CHNS/O analyzer (ThermoFisher Scientific). Pre-catalysts **A**, **B**, **C**, oxidant **7**, durene, Iron(II) phthalocyanine **8**, sodium pyruvate (**SP**), isosorbide **2**, starting aldehydes and amines for imines synthesis were purchased from commercial source and used as received. Liquid aldehydes and bases (DBU, Et_3N) were freshly distilled before their utilization. Molecular sieves (4 Å, powder; 5 Å, 1.6 mm particle size) were activated at 300 °C for 24 h and next cooled to room temperature under vacuum. Supported pre-catalyst **D** was synthesized according to a literature procedure^[20b] and the relative degree of functionalization was detected via elemental analysis. Imines **1a–i** were synthesized as described below.

General procedure for the synthesis of imines **1a–i**

A stirred mixture of amine (7 mmol), aromatic aldehyde (7 mmol) and 5 Å molecular sieves (1.6 mm particle size, 1 g/mmol) in anhydrous toluene (130 mL) was refluxed for 16 h under Argon atmosphere. After complete conversion of the starting material, detected by NMR analysis, molecular sieves were filtered off and the solvent was removed under vacuum to furnish the crude aldimine. Trituration with 2-propanol or cyclohexane furnished the purified imine **1** with almost quantitative yield.

Screening of reaction conditions with diquinone **7** as oxidant (Table 1)

A stirred mixture of imine **1a** (48 mg, 0.2 mmol), isosorbide **2** (88 mg, 0.6 mmol), oxidant **7** (82 mg, 0.2 mmol), durene (27 mg, 0.2 mmol) and the stated pre-catalyst (from 0.01 to 0.04 mmol) in the selected anhydrous solvent (2 mL) was degassed under vacuum and saturated with argon (by an Ar-filled balloon) three times. Then, DBU was added (from 0.04 to 0.06 mmol), and the reaction mixture was stirred at room temperature for the stated time. Yields of **3a**, **4a** and **5a** were evaluated by ^1H NMR analysis of the crude reaction mixture (durene as internal standard).

Screening of reaction conditions under aerobic conditions (Table 2)

Entries 1–3. A stirred mixture of imine **1a** (48 mg, 0.2 mmol), isosorbide **2** (88 mg, 0.6 mmol), oxidant **7** (8 mg, 0.02 mmol), ETM **8** (6 mg, 0.01 mmol), durene (27 mg, 0.2 mmol), 4 Å molecular sieves (0.2 g, powder) and the stated pre-catalyst (from 0.01 to 0.02 mmol) in the selected anhydrous solvent (2 mL) was stirred under an air atmosphere (by a compressed air-filled balloon). Then, DBU was added (from 0.04 to 0.05 mmol), and the reaction mixture was stirred at room temperature for the stated time. Yields of **3a**, **4a**, **5a** and **6a** were evaluated by ^1H NMR analysis of the crude reaction mixture (durene as internal standard).

Entry 4. A stirred mixture of imine **1a** (48 mg, 0.2 mmol), isosorbide **2** (88 mg, 0.6 mmol), durene (27 mg, 0.2 mmol), 4 Å molecular sieves (0.2 g, powder) and pre-catalyst **A** (4.5 mg, 0.02 mmol) in anhydrous DCM (2 mL) was stirred under an O_2 atmosphere (by an O_2 filled balloon, 1 bar). Then, DBU was added (7.5 μL , 0.05 mmol), and the reaction mixture was stirred at room temperature for 16 h. Yields of **3a**, **4a**, **5a** and **6a** were evaluated by ^1H NMR analysis of the crude reaction mixture (durene as internal standard).

Entries 5–9. A stirred mixture of imine **1a** (48 mg, 0.2 mmol), isosorbide **2** (88 mg, 0.6 mmol), sodium pyruvate (**SP**) (22 mg, 0.2 mmol), durene (27 mg, 0.2 mmol), 4 Å molecular sieves (0.2 g, powder) and the stated pre-catalyst (0.04 mmol) in the selected anhydrous solvent (2 mL) was stirred under an air atmosphere (by a

compressed air-filled balloon). Then, the selected base was added (from 0.06 to 0.3 mmol), and the reaction mixture was stirred at room temperature for the stated time. Yields of **3a**, **4a**, **5a** and **6a** were evaluated by ^1H NMR analysis of the crude reaction mixture (durene as internal standard).

General procedure for the regioselective synthesis of *exo*-MIIIs **3a–i**

A stirred mixture of imine **1** (0.2 mmol), isosorbide **2** (88 mg, 0.6 mmol), oxidant **7** (82 mg, 0.2 mmol), and precatalyst **A** (2.3 mg, 0.01 mmol) in anhydrous DCM (2 mL) was degassed under vacuum and saturated with Argon (by an Ar-filled balloon) three times. Then, DBU was added (6 μL , 0.04 mmol), and the reaction mixture was stirred at room temperature until almost complete imine consumption was detected (NMR analysis). The reaction mixture was then diluted with DCM (10 mL) and washed with water (3 \times 5 mL). The organic layer was dried (Na_2SO_4), concentrated, and eluted from a column of silica gel with a suitable elution system to give, in order of elution, alcohol **7'**, diimidate **5**, amide **6**, *exo*-MII **3** and *endo*-MII **4**.

General procedure for the regioselective synthesis of *endo*-MIIIs **4a–i**

A stirred mixture of imine **1** (0.2 mmol), isosorbide **2** (88 mg, 0.6 mmol), oxidant **7** (82 mg, 0.2 mmol), and precatalyst **B** (7 mg, 0.02 mmol) in anhydrous NMP (2 mL) was degassed under vacuum and saturated with Argon (by an Ar-filled balloon) three times. Then, DBU was added (7.5 μL , 0.05 mmol), and the reaction mixture was stirred at room temperature until almost complete imine consumption was detected (NMR analysis). The reaction mixture was then diluted with EtOAc (10 mL) and washed with water (3 \times 5 mL). The organic layer was dried (Na_2SO_4), concentrated, and eluted from a column of silica gel with a suitable elution system to give, in order of elution, alcohol **7'**, *exo*-MII **3**, and *endo*-MII **4**.

Procedure for oxidant **7** recycle

The quantitative recycle of diquinone **7** was conducted stirring the isolated **7'** alcohol (75 mg, 0.18 mmol) with **8** (11 mg, 0.02 mmol) in THF (2 mL) under air atmosphere (1 atm, balloon) for 16 h. Filtration over celite and concentration under reduced pressure afforded diquinone **7** as a red amorphous solid (65 mg, 90%).

Acknowledgements

We gratefully acknowledge the University of Ferrara (fondi FAR) for financial support. Thanks are also given to Morgana Montanari for her valuable synthetic contribution, to Paolo Formaglio for NMR experiments and to Ercolina Bianchini for elemental analyses. Open Access funding provided by Università degli Studi di Ferrara within the CRUI-CARE Agreement.

Conflict of Interest

The authors declare no conflict of interest.

Data Availability Statement

The data that support the findings of this study are available in the supplementary material of this article.

Keywords: N-heterocyclic carbene · Nitrogen heterocycles · Organocatalysis · Regioselectivity · Renewable Resources

- [1] For some recent papers, see: a) H. Kwon, Y. Kim, K. Park, S. A. Choi, S.-H. Son, Y. Byun, *Bioorg. Med. Chem. Lett.* **2016**, *26*, 310–314; b) Z. Han, P. K. W. Harris, P. Karmakar, T. Kim, B. Y. Owusu, S. A. Wildman, L. Klampfer, J. W. Janetka, *ChemMedChem* **2016**, *11*, 585–599; c) V. C. Damalanka, S. A. Wildman, J. W. Janetka, *MedChemComm* **2019**, *10*, 1646–1655; d) M. A. Morsy, E. M. Ali, M. Kandeel, K. N. Venugopala, A. B. Nair, K. Greish, M. El-Daly, *Antibiotics* **2020**, *9*, 221; e) X.-J. Zheng, C.-S. Li, M.-Y. Cui, Z.-W. Song, X.-Q. Bai, C.-W. Liang, H.-Y. Wang, T.-Y. Zhang, *Bioorg. Med. Chem. Lett.* **2020**, *30*, 127237; f) S. Castro-Sánchez, J. Zaldivar-Diez, E. Luengo, M. G. López, C. Gil, A. Martínez, I. Lastres-Becker, *Neurobiol. Aging* **2020**, *96*, 148–154; g) S. Harisha, K. Jathi, S. M. Prasanna, H. Joy Hoskeri, *J. Mol. Struct.* **2020**, *1218*, 128477.
- [2] For selected reviews, see: a) M. N. Bhoi, M. A. Borad, H. D. Patel, *Synth. Commun.* **2014**, *44*, 2427–2457; b) R. S. Keri, M. R. Patil, S. A. Patil, S. Budagumpi, *Eur. J. Med. Chem.* **2015**, *89*, 207–251; c) A. Rouf, C. Tanyeli, *Eur. J. Med. Chem.* **2015**, *97*, 911–927; d) S. Sulthana, P. Pandian, *J. Drug Delivery Ther.* **2019**, *9*, 505–509; e) M. B. Elamin, A. A. E. S. A. Elaziz, E. M. Abdallah, *Int. J. Res. Pharm. Sci.* **2020**, *11*, 3309–3315; f) Y. I. Asiri, A. Alsayari, A. B. Muhsinah, Y. N. Mabkhot, M. Z. Hassan, *J. Pharm. Pharmacol.* **2020**, *72*, 1459–1480.
- [3] S. Noël, S. Cadet, E. Gras, C. Hureau, *Chem. Soc. Rev.* **2013**, *42*, 7747–7762.
- [4] Y. Hu, J. B. MacMillan, *Org. Lett.* **2011**, *13*, 6580–6583.
- [5] I. Argyropoulou, A. Geronikaki, P. Vicini, F. Zani, *Arkivoc* **2009**, (vi), 89–102.
- [6] a) A. Doble, *Neurology* **1996**, *47*, S233–S241; b) H. M. Bryson, B. Fulton, P. Benfield, *Drugs* **1996**, *52*, 549–563; c) P. Jimonet, F. Audiau, M. Barreau, J.-C. Blanchard, A. Boireau, Y. Bour, M.-A. Coléno, A. Doble, G. Doerflinger, C. Do Huu, M.-H. Donat, J. M. Duchesne, P. Ganil, C. Guérémy, E. Honoré, B. Just, R. Kerphirique, S. Gontier, P. Hubert, P. M. Laduron, J. Le Blevet, M. Meunier, J.-M. Miquet, C. Nemecek, M. Pasquet, O. Piot, J. Pratt, J. Rataud, M. Reibaud, J.-M. Stutzmann, S. Mignani, *J. Med. Chem.* **1999**, *42*, 2828–2843.
- [7] a) C. A. Mathis, Y. Wang, D. P. Holt, G.-F. Huang, M. L. Debnath, W. E. Klunk, *J. Med. Chem.* **2003**, *46*, 2740–2754; b) W. E. Klunk, H. Engler, A. Nordberg, Y. Wang, G. Blomqvist, D. P. Holt, M. Bergström, I. Savitcheva, G.-F. Huang, S. Estrada, B. Ausén, M. L. Debnath, J. Barletta, J. C. Price, J. Sandell, B. J. Lopresti, A. Wall, P. Koivisto, G. Antoni, C. A. Mathis, B. Långström, *Ann. Neurol.* **2004**, *55*, 306–319; c) W. E. Klunk, C. A. Mathis, J. C. Price, B. J. Lopresti, S. T. Dekosky, *Brain* **2006**, *129*, 2805–2807; d) Y. Omachi, K. Ito, K. Arima, H. Matsuda, Y. Nakata, M. Sakata, N. Sato, K. Nakagome, N. Motohashi, *Psychiatry Clin. Neurosci.* **2015**, *69*, 741–751; e) A. D. Cohen, *Technol. Innov.* **2016**, *18*, 51–61; f) Q. Yan, K. Nho, J. L. Del-Aguila, X. Wang, S. L. Risacher, K.-H. Fan, B. E. Snitz, H. J. Aizenstein, C. A. Mathis, O. L. Lopez, F. Y. Demirci, E. Feingold, W. E. Klunk, A. J. Saykin, C. Cruchaga, M. I. Kamboh, *Mol. Psychiatry* **2021**, *26*, 309–321; g) K. Kitajima, K. Abe, M. Takeda, H. Yoshikawa, M. Ohigashi, K. Osugi, H. Koyama, K. Yamakado, *Medicine* **2021**, *100*, e23969.
- [8] Y. Miyake, J. Sakai, M. Shibata, N. Yonekura, I. Miura, K. Kumakura, K. Nagayama, *J. Pestic. Sci.* **2005**, *30*, 390–396.
- [9] a) H. Liu, H. Lu, Z. Zhou, S. Shimizu, Z. Li, N. Kobayashi, Z. Shen, *Chem. Commun.* **2015**, *51*, 1713–1716; b) S. J. Carrington, I. Chakraborty, J. M. L. Bernard, P. K. Mascharak, *Inorg. Chem.* **2016**, *55*, 7852–7858; c) Y.-X. Hu, X. Xia, W.-Z. He, Z.-J. Tang, Y.-L. Lv, X. Li, D.-Y. Zhang, *Org. Electron.* **2019**, *66*, 126–135.
- [10] a) N. P. Prajapati, R. H. Vekariya, M. A. Borad, H. D. Patel, *RSC Adv.* **2014**, *4*, 60176–60208; b) X. Gao, J. Liu, X. Zuo, X. Feng, Y. Gao, *Molecules* **2020**, *25*, 1675.
- [11] W. Li, J. Lv, Y. R. Chi, *Tetrahedron* **2021**, *94*, 132311.
- [12] a) C. E. I. Knappke, A. Imami, A. Jacobi von Wangelin, *ChemCatChem* **2012**, *4*, 937–941; b) S. De Sarkar, A. Biswas, R. C. Samanta, A. Studer, *Chem. Eur. J.* **2013**, *19*, 4664–4678; c) K. Dzieszowski, Z. Rafiński, *Catalysts* **2018**, *8*, 549; d) A. Axelsson, L. Ta, H. Sundén, *Synlett* **2017**, *28*, 873–878; e) G. Di Carmine, D. Ragno, A. Brandolese, O. Bortolini, D. Pecorari, F. Sabuzi, A. Mazzanti, A. Massi, *Chem. Eur. J.* **2019**, *25*, 7469–7474; f) A. Brandolese, D. Ragno, C. Leonardi, G. Di Carmine, O. Bortolini, C. De Risi, A. Massi, *Eur. J. Org. Chem.* **2020**, *16*, 2439–2447; g) T. Pavithra, E. S. Devi, C. U. Maheswari, *Asian J. Org. Chem.* **2021**, *10*, 1861–1883.
- [13] Q. Zhou, S. Liu, M. Ma, H.-Z. Cui, X. Hong, S. Huang, J.-F. Zhang, X.-F. Hou, *Synthesis* **2018**, *50*, 1315–1322.
- [14] S. Premaletha, A. Ghosh, S. Joseph, S. R. Yetra, A. T. Biju, *Chem. Commun.* **2017**, *53*, 1478–1481.
- [15] G. Wang, Z. Fu, W. Huang, *Org. Lett.* **2017**, *19*, 3362–3365.
- [16] G. Wang, C. Wei, X. Hong, Z. Fu, W. Huang, *Green Chem.* **2020**, *22*, 6819–6826.
- [17] a) G. D. Kini, R. K. Robins, T. L. Avery, *J. Med. Chem.* **1989**, *32*, 1447–1449; b) L. M. Deck, D. L. Vender Jagt, R. E. Royer, *J. Med. Chem.* **1991**, *34*, 3301–3305; c) R. E. Royer, R. G. Mills, L. M. Deck, G. J. Metz, D. L. Vander Jagt, *Pharmacol. Res.* **1991**, *24*, 407–412; d) S. G. Hegde, R. D. Bryant, L. F. Lee, S. K. Parrish, W. B. Parker, *ACS Symp. Ser.* **1995**, *584*, 60–69; e) M. Boukthir, F. Chabchouba, *RRJCHEM* **2017**, *6*, 22–33; f) Y. Liu, X. Hu, Y. Wu, W. Zhang, X. Chen, X. You, L. Hu, *Eur. J. Med. Chem.* **2018**, *150*, 771–782; g) C. C. Santos, J. R. Lionel, R. B. Peres, M. M. Batista, P. B. da Silva, G. M. de Oliveira, C. F. da Silva, D. G. Batista, S. M. O. Souza, C. H. Andrade, B. J. Neves, R. C. Braga, D. A. Patrick, S. M. Bakunova, R. R. Tidwell, M. de N. C. Soeiro, *Antimicrob. Agents Chemother.* **2018**, *62*, e02205–17.
- [18] a) *The Chemistry of Amidines and Imidates*, Vol. 2 (Eds.: S. Patai, Z. Rappoport), Wiley, Chichester (UK), **1991**; b) R. Matsubara, F. Berthiol, S. Kobayashi, *J. Am. Chem. Soc.* **2008**, *130*, 1804–1805; c) T. R. M. Rauws, B. U. W. Maes, *Chem. Soc. Rev.* **2012**, *41*, 2463–2497; d) Z. Wang, S. Sueki, M. Kanai, Y. Kuninobu, *Org. Lett.* **2016**, *18*, 2459–2462; e) H. Wang, M. L. Lorion, L. Ackermann, *ACS Catal.* **2017**, *7*, 3430–3433; f) R. Thakur, Y. Jaiswal, A. Kumar, *Org. Biomol. Chem.* **2019**, *17*, 9829–9843; g) W. Guo, M. Zhao, W. Tan, L. Zheng, K. Tao, X. Fan, *Org. Chem. Front.* **2019**, *6*, 2120–2141.
- [19] a) J. S. Pap, B. Kripli, V. Banyai, M. Giorgi, L. Korecz, T. Gajda, D. Árus, J. Kaizer, G. Speier, *Inorg. Chim. Acta* **2011**, *376*, 158–169; b) T. Váradi, J. S. Pap, M. Giorgi, L. Párkányi, T. Csay, G. Speier, J. Kaizer, *Inorg. Chem.* **2013**, *52*, 1559–1569; c) M. A. Potopnyk, D. Volyniuk, R. Luboradzki, M. Ceborska, I. Hladka, Y. Danyliv, J. V. Gražulevičius, *J. Org. Chem.* **2019**, *84*, 5614–5626.
- [20] a) A. Brandolese, D. Ragno, G. Di Carmine, T. Bernardi, O. Bortolini, P. P. Giovannini, O. G. Pandoli, A. Altomare, A. Massi, *Org. Biomol. Chem.* **2018**, *16*, 8955–8964; b) D. Ragno, A. Brandolese, D. Urbani, G. Di Carmine, C. De Risi, O. Bortolini, P. P. Giovannini, A. Massi, *React. Chem. Eng.* **2018**, *3*, 816–825; c) D. Ragno, G. Di Carmine, A. Brandolese, O. Bortolini, P. P. Giovannini, G. Fantin, M. Bertoldo, A. Massi, *Chem. Eur. J.* **2019**, *25*, 14701–14710; d) D. Ragno, A. Brandolese, G. Di Carmine, S. Buoso, G. Belletti, C. Leonardi, O. Bortolini, M. Bertoldo, A. Massi, *Chem. Eur. J.* **2021**, *27*, 1839–1848; e) D. Ragno, C. Leonardi, G. Di Carmine, O. Bortolini, A. Brandolese, C. De Risi, A. Massi, *ACS Sustainable Chem. Eng.* **2021**, *9*, 8295–8305; f) D. Ragno, G. Di Carmine, M. Vannini, O. Bortolini, D. Perrone, S. Buoso, M. Bertoldo, A. Massi, *Polym. Chem.* **2022**, *13*, 1350–1358.
- [21] a) F. Delbecq, M. R. Khodadadi, D. Rodriguez Padron, R. Varma, C. Len, *J. Mol. Catal.* **2020**, *482*, 110648; b) I. Bonnin, R. Mereau, T. Tassaing, K. De Oliveira Vigier, *Beilstein J. Org. Chem.* **2020**, *16*, 1713–1721.
- [22] a) M. Rose, R. Palkovits, *ChemSusChem* **2012**, *5*, 167–176; b) C. Dussonne, T. Delaunay, V. Wiatz, H. Wyart, I. Suisse, M. Sauthier, *Green Chem.* **2017**, *19*, 5332–5344.
- [23] a) S. Meninno, *ChemSusChem* **2020**, *13*, 439–468; b) S. Jopp, *Eur. J. Org. Chem.* **2020**, *2020*, 6418–6428.
- [24] a) R. Storbeck, M. Rehahn, M. Ballauff, *Makromol. Chem.* **1993**, *194*, 53–64; b) R. Storbeck, M. Ballauff, *J. Appl. Polym. Sci.* **1996**, *59*, 1199–1202; c) A. Gandini, D. Coelho, M. Gomes, B. Reis, A. Silvestre, *J. Mater. Chem.* **2009**, *19*, 8656–8664; d) J. Wu, P. Eduard, L. Jasinska-Walc, A. Rozanski, B. A. J. Noordover, D. S. van Es, C. E. Koning, *Macromolecules* **2013**, *46*, 384–394; e) J. M. Sadler, A.-P. T. Nguyen, F. R. Toulan, J. P. Szabo, G. R. Palmese, C. Scheck, S. Lutgen, J. J. La Scala, *J. Mater. Chem. A* **2013**, *1*, 12579–12586; f) J. Chen, J. Wu, J. Qi, H. Wang, *ACS Sustainable Chem. Eng.* **2019**, *7*, 1061–1071; g) Y. Chebbi, N. Kasmi, M. Majdoub, P. Cerruti, G. Scarinzi, M. Malinconico, G. Dal Poggetto, G. Z. Papageorgiou, D. N. Bikiaris, *ACS Sustainable Chem. Eng.* **2019**, *7*, 5501–5514; h) M. Al-Naji, H. Schlaad, M. Antonietti, *Macromol. Rapid Commun.* **2020**, *42*, 2000485; i) O. Gómez-de-Miranda-Jiménez-de-Aberasturi, A. Centeno-Pedrazo, S. Prieto Fernández, R. Rodríguez Alonso, S. Medel, J. María Cuevas, L. G.

- Monsegue, S. De Wildeman, E. Benedetti, D. Klein, H. Henneken, J. R. Ochoa-Gómez, *Green Chem. Lett. Rev.* **2021**, *14*, 534–544.
- [25] a) B. Yin, M. Hakkarainen, *J. Appl. Polym. Sci.* **2011**, *119*, 2400–2407; b) C. Cui, Y. Zhen, J. Qu, B. Chen, T. Tan, *RSC Adv.* **2016**, *6*, 11959–11966.
- [26] a) A. Lavergne, L. Moity, V. Molinier, J.-M. Aubry, *RSC Adv.* **2013**, *3*, 5997–6007; b) T. Vijai Kumar Reddy, G. Sandhya Rani, R. B. N. Prasad, B. L. A. Prabhavathi Devi, *RSC Adv.* **2015**, *5*, 40997–41005; c) C. Stoer, C. Nieendick, M. Weissenegger, D. Prinz, M. Winzek, J. Schoss, M. Dierker, N. Boyxen, U. Griesbach, W. Seipel, W. Mauer, WO 2016008747A1, **2015**.
- [27] a) U. Abshagen, S. Spoerl-Radun, *Eur. J. Clin. Pharmacol.* **1981**, *19*, 423–429; b) S.-G. Zhu, J.-T. Yang, G.-M. Zhang, C.-F. Chen, F.-L. Zhang, *Org. Process Res. Dev.* **2018**, *22*, 991–995.
- [28] a) L. Matt, J. Parve, O. Parve, T. Pehk, T. H. Pham, I. Liblikas, L. Vares, P. Jannasch, *ACS Sustainable Chem. Eng.* **2018**, *6*, 17382–17390; b) S. Laanesoo, O. Bonjour, J. Parve, O. Parve, L. Matt, L. Vares, P. Jannasch, *Biomacromolecules* **2021**, *22*, 640–648.
- [29] J. F. Gilmer, L. M. Moriarty, D. F. McCafferty, J. M. Clancy, *Eur. J. Pharm. Sci.* **2001**, *14*, 221–227.
- [30] a) O. Bortolini, A. Cavazzini, P. Dambrosio, P. P. Giovannini, L. Caciolli, A. Massi, S. Pacifico, D. Ragno, *Green Chem.* **2013**, *15*, 2981–2992; b) D. Ragno, G. Di Carmine, A. Brandolese, O. Bortolini, P. P. Giovannini, A. Massi, *ACS Catal.* **2017**, *7*, 6365–6375; c) C. De Risi, O. Bortolini, A. Brandolese, G. Di Carmine, D. Ragno, A. Massi, *React. Chem. Eng.* **2020**, *5*, 1017–1052; d) G. Di Carmine, D. Ragno, A. Massi, C. D'Agostino, *Org. Lett.* **2020**, *22*, 4927–4931.
- [31] a) O. Bortolini, C. Chiappe, M. Fogagnolo, P. P. Giovannini, A. Massi, C. S. Pomelli, D. Ragno, *Chem. Commun.* **2014**, *50*, 2008–2011; b) O. Bortolini, C. Chiappe, M. Fogagnolo, A. Massi, C. S. Pomelli, *J. Org. Chem.* **2017**, *82*, 302–312.
- [32] a) A. Patra, A. James, T. K. Das, A. T. Biju, *J. Org. Chem.* **2018**, *83*, 14820–14826; b) T. K. Das, K. Madica, J. Krishnan, U. K. Marelli, A. T. Biju, *J. Org. Chem.* **2020**, *85*, 5114–5121; c) X. Yang, Y. Xie, J. Xu, S. Ren, B. Mondal, L. Zhou, W. Tian, X. Zhang, L. Hao, Z. Jin, Y. R. Chi, *Angew. Chem. Int. Ed.* **2021**, *60*, 7906–7912; d) G. Wang, Q.-C. Zhang, C. Wei, Y. Zhang, L. Zhang, J. Huang, D. Wei, Z. Fu, W. Huang, *Angew. Chem. Int. Ed.* **2021**, *60*, 7913–7919.
- [33] a) G. Wang, W. Hu, Z. Hu, Y. Zhang, W. Yao, L. Zi, Z. Fu, W. Huang, *Green Chem.* **2018**, *20*, 3302–3307; b) K. Satyam, B. Harish, J. B. Nanubolu, S. Suresh, *Chem. Commun.* **2020**, *56*, 2803–2806; c) J. Ramarao, S. Yadav, K. Satyam, S. Suresh, *RSC Adv.* **2022**, *12*, 7621–7625.
- [34] J. Piera, J.-E. Bäckvall, *Angew. Chem. Int. Ed.* **2008**, *47*, 3506–3523; *Angew. Chem.* **2008**, *120*, 3558–3576.
- [35] A. Axelsson, A. Antoine-Michard, H. Sundén, *Green Chem.* **2017**, *19*, 2477–2481.

Manuscript received: April 27, 2022
Revised manuscript received: May 19, 2022
Accepted manuscript online: May 23, 2022